Smart Structures and Systems, *Vol. 23, No. 4 (2019) 387-392*
DOI: https://doi.org/10.12989/sss.2019.23.4.387

Vibration response of smart concrete plate based on numerical methods

Reza Taherifar*[1], Farhad Chinaei[2], Shahram Ghaedi Faramoushjan[2], Mohammad Hossein Nasr Esfahani[3], Shabnam Nasr Esfahani[4] and Maryam Mahmoudi[5]

[1]*Department of Civil Engineering, Meymeh Branch, Islamic Azad University, Meymeh Iran*
[2]*Department of Civil and Mineral Engineering, Meymeh Branch, Islamic Azad University, Meymeh Iran*
[3]*Department of Mathematics, Faculty of Basic Science, Meymeh Branch, Islamic Azad University, Meymeh Iran*
[4]*Department of Electrical Engineering, Meymeh Branch, Islamic Azad University, Meymeh Iran*
[5]*Department of Computer Engineering, Meymeh Branch, Islamic Azad University, Meymeh Iran*

(Received February 11, 20198, Revised March 28, 2019, Accepted March 30, 2019)

Abstract. This research deals with the vibration analysis of embedded smart concrete plate reinforced by zinc oxide (ZnO). The effective material properties of structure are considered based on mixture rule. The elastic medium is simulated by orthotropic visco-Pasternak medium. The motion equations are derived applying Sinusoidal shear deformation theory (SSDT). The differential quadrature (DQ) method is applied for calculating frequency of structure. The effects of different parameters such as volume percent of ZnO, boundary conditions and geometrical parameters on the frequency of system are shown. The results are compared with other published works in the literature. Results indicate that the ZnO have an important role in frequency of structure.

Keywords: vibration; FG-CNT; smart concrete plate; SSDT; visco-elastic

1. Introduction

Nanocomposite materials are composed of different functional components such as polymer, nanoparticle and ligands, with at least one component having nanometer dimensions. Typically, the dispersion of nanoparticles in polymer matrices is problematic and the nanoparticles tend to phase separate or aggregate in the polymer matrix. Nanoparticle agglomeration and phase separation from the host polymer usually results in poor process ability of films and a high defect density. Moreover, physical properties of the composite material are very sensitive to particle dispersion within the nanocomposite (Mori and Tanaka 1973).

Mechanical analysis of nano\smart concrete plate were taken up by several researchers lately. A finite element model based on an improved higher order zigzag plate theory was developed by Pandit *et al*. (2009) for bending and vibration response of soft core smart concrete plate. Buckling and free vibration of magneto-electro-elastic nanoplate resting on Pasternak foundation was presented by Li *et al.* (2014) based on Mindlin theory. Applying different shear deformable plate theories, Kiani (2014) carried out the free vibration of conducting nanosmart concrete plate exposed to unidirectional in-plane magnetic fields. Ke *et al.* (2015) presented free vibration of piezoelectric nanosmart concrete plate using differential quadrature method (DQM). Asimple four-variable trigonometric shear deformation theory considering the effects of transverse shear deformation and rotary inertia was evaluated by Atteshamuddin and Yuwaraj (2017) for the free vibration analysis of antisymmetric laminated composite and soft core smart concrete plate. The magneto-rheological visco-elastomer (MRVE) was used by Ying *et al*. (2017) as a smart core to control the stochastic micro-vibration of a plate with supported mass.

With respect to the developed works for nanocomposite structures, there are many works in recent years. Nonlinear bending of FG-CNTRC smart concrete plate was presented by Shen (2009), who considered the size-dependent and temperature dependent material properties of single-wall CNTs. The bending and free flexural vibration behavior of smart concrete plate with CNT reinforced face sheets were investigated by Natarajan *et al*. (2014). Abdollahzadeh Shahrbabaki and Alibeigloo (2014) studied the three-dimensional free vibration of CNT reinforced composite rectangular orthotropic smart concrete plate with various boundary conditions. Four-unknown quasi-3D shear deformation theory for advanced composite smart concrete plate was investigated by Mantari and Guedes Soares (2014). Rafiee *et al.* (2014) worked on non-linear dynamic stability of piezoelectric FG-CNTRC smart concrete plate with initial geometric imperfection. Wattanasakulpong and Chaikittiratana (2015) carried out the exact solutions for static and dynamic analyses of CNTRC smart concrete plate with Pasternak elastic foundation. Phung-Van *et al.* (2017) presented the iso-geometric analysis of FG-CNTRC smart concrete plate using higher-order shear deformation theory. Chetan *et al.* (2017) studied modelling of the interfacial

*Corresponding author, Dr.
E-mail: rtf_55@yahoo.com

ISSN: 1738-1584 (Print), 1738-1991 (Online)

damping due to nanotube agglomerations in nanocomposites.

Here, a model for vibration of smart concrete plate reinforced with ZnO is studied. The surrounding elastic medium is simulated by orthotropic visco-Pasternak foundation. The mixture rule is applied for obtaining the equivalent material properties of structure. The motion equations are obtained using SSDT and energy method considering size effects. DQ method is used to calculate the resonance frequency of structure. The effects of different parameters such as volume percent of ZnO, boundary conditions and geometrical parameters on the frequency of system are elucidated.

2. Mixture rule

As shown in Fig. 1, a concrete plate with length a, width b and thickness h is considered. The plate is surrounded by an orthotropic elastomeric medium which is simulated by K_W, $K_{g\xi}$ and $K_{g\eta}$ correspond Winkler foundation parameter, shear foundation parameters in ξ and η directions, respectively.

In order to obtain the equivalent material properties two-phase Nanocomposites (i.e., polymer as matrix and ZnO as reinforcer), the rule of mixture is applied. According to mixture rule, the effective Young and shear moduli of CNTRC plate can be written as (Shen 2009)

$$\mathrm{E}_{11}=\eta_1\mathrm{V}_{\mathrm{ZnO}}\mathrm{E}_{\mathrm{r11}}+(1-\mathrm{V}_{\mathrm{ZnO}})\mathrm{E}_{\mathrm{m}}, \tag{1}$$

$$\frac{\eta_2}{\mathrm{E}_{22}}=\frac{\mathrm{V}_{\mathrm{ZnO}}}{\mathrm{E}_{\mathrm{r22}}}+\frac{(1-\mathrm{V}_{\mathrm{ZnO}})}{\mathrm{E}_{\mathrm{m}}}, \tag{2}$$

$$\frac{\eta_3}{\mathrm{G}_{12}}=\frac{\mathrm{V}_{\mathrm{ZnO}}}{\mathrm{G}_{\mathrm{r12}}}+\frac{(1-\mathrm{V}_{\mathrm{ZnO}})}{\mathrm{G}_{\mathrm{m}}}, \tag{3}$$

where E_{r11}, E_{r22} and G_{r11} indicate the Young's moduli and shear modulus of ZnO, respectively, and E_m, G_m represent the corresponding properties of the isotropic matrix.

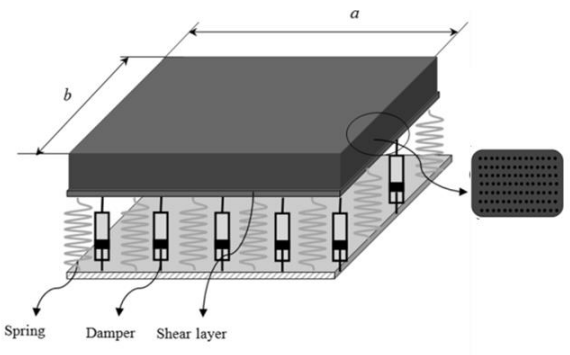

Fig. 1 Configurations of the smart concrete plate

The scale-dependent material properties, η_j (j= 1, 2, 3), can be calculated by matching the effective properties of structure obtained from the MD simulations with those from the rule of mixture. $\mathrm{V}_{\mathrm{ZnO}}$ and V_m are the volume fractions of the ZnO and matrix, respectively, which the sum of them equals to unity. The uniform distribution of the ZnO along the thickness direction of the smart concrete plate take the following forms

$$\mathrm{UD}: \quad \mathrm{V}_{\mathrm{ZnO}}=\mathrm{V}_{\mathrm{ZnO}}^{*}, \tag{4}$$

where

$$\mathrm{V}_{\mathrm{ZnO}}^{*}=\frac{\mathrm{w}_{\mathrm{Zno}}}{\mathrm{w}_{\mathrm{Zno}}+(\rho_{\mathrm{ZnO}}/\rho_{\mathrm{m}})-(\rho_{\mathrm{ZnO}}/\rho_{\mathrm{m}})\mathrm{w}_{\mathrm{ZnO}}}, \tag{5}$$

where $\mathrm{w}_{\mathrm{ZnO}}$, ρ_m and ρ_{ZnO} are the mass fraction of the ZnO, the densities of the matrix and ZnO, respectively.

3. Sinusoidal theories

The stress relations are

$$\sigma_{ij}=C_{ijkl}\varepsilon_{kl}, \tag{6}$$

$$\begin{Bmatrix}\sigma_{xx}\\ \sigma_{yy}\\ \sigma_{yz}\\ \sigma_{zx}\\ \sigma_{xy}\end{Bmatrix}=\begin{bmatrix}C_{11} & C_{12} & 0 & 0 & 0\\ C_{21} & C_{22} & 0 & 0 & 0\\ 0 & 0 & C_{44} & 0 & 0\\ 0 & 0 & 0 & C_{55} & 0\\ 0 & 0 & 0 & 0 & C_{66}\end{bmatrix}\begin{Bmatrix}\varepsilon_{xx}\\ \varepsilon_{yy}\\ \gamma_{yz}\\ \gamma_{xz}\\ \gamma_{xy}\end{Bmatrix}, \tag{7}$$

where C_{ij} denotes elastic coefficients. Noted that C_{ij} may be obtained using rule of mixture. Based on the SSDT, the displacement field can be written as (Thai and Vo 2013)

$$U_1(x,y,z,t)=U(x,y,t)-z\frac{\partial W_b}{\partial x}-f\frac{\partial W_s}{\partial x}, \tag{8}$$

$$U_2(x,y,z,t)=V(x,y,t)-z\frac{\partial W_b}{\partial y}-f\frac{\partial W_s}{\partial y}, \tag{9}$$

$$U_3(x,y,z,t)=W_b(x,y,t)+W_s(x,y,t), \tag{10}$$

where $f=z-(\frac{h}{\pi}\sin\frac{\pi z}{h})$ .The von Kármán strains by utilizing SSDT can be described as

$$\varepsilon_{xx}=\frac{\partial U}{\partial x}-z\frac{\partial^2 W_b}{\partial x^2}-f\frac{\partial^2 W_s}{\partial x^2}, \tag{11}$$

$$\varepsilon_{yy}=\frac{\partial V}{\partial y}-z\frac{\partial^2 W_b}{\partial y^2}-f\frac{\partial^2 W_s}{\partial y^2}, \tag{12}$$

$$\varepsilon_{xy} = \frac{\partial U}{\partial y} + \frac{\partial V}{\partial x} - 2z\frac{\partial^2 W_b}{\partial x \partial y} - 2f\frac{\partial^2 W_S}{\partial x \partial y}, \quad (13)$$

$$\gamma_{yz} = g\frac{\partial W_s}{\partial y}, \quad (14)$$

$$\gamma_{xz} = g\frac{\partial W_s}{\partial x}, \quad (15)$$

where $g = 1 - \frac{df}{dz} = \cos(\frac{\pi z}{h})$.

4. Motion equations

The potential energy of structure can be written as

$$U = \frac{1}{2}\int_A \int_{-\frac{h}{2}}^{\frac{h}{2}} \left(\sigma_{xx}\varepsilon_{xx} + \sigma_{yy}\varepsilon_{yy} + \sigma_{xy}\gamma_{xy} + \sigma_{xz}\gamma_{xz} + \sigma_{yz}\gamma_{yz}\right) dz dA \quad (16)$$

Substituting Eqs. (11)-(15) into Eq. (16) leads to

$$\begin{aligned} U = \frac{1}{2}\int_A \Bigg(& N_{xx}\frac{\partial u}{\partial x} + N_{xy}\frac{\partial u}{\partial y} + N_{xy}\frac{\partial v}{\partial x} \\ & + N_{yy}\frac{\partial v}{\partial y} + Q_x\frac{\partial w_s}{\partial x} + Q_y\frac{\partial w_s}{\partial y} - M_{xxS}\frac{\partial^2 w_s}{\partial x^2} \\ & - M_{yyS}\frac{\partial^2 w_s}{\partial y^2} - 2M_{xyS}\frac{\partial^2 w_s}{\partial y \partial x} - M_{xxB}\frac{\partial^2 w_b}{\partial x^2} \\ & - M_{yyB}\frac{\partial^2 w_b}{\partial y^2} - 2M_{xyB}\frac{\partial^2 w_b}{\partial y \partial x}\Bigg) \mathrm{dA}, \end{aligned} \quad (17)$$

where N, M and Q are the stress resultant–displacement can be defined by

$$\left(N_{xx}, N_{yy}, N_{xy}\right) = \int_{-\frac{h}{2}}^{\frac{h}{2}} (\sigma_{xx}, \sigma_{yy}, \sigma_{xy}) dz, \quad (18)$$

$$\left(M_{xxB}, M_{yyB}, M_{xyB}\right) = \int_{-\frac{h}{2}}^{\frac{h}{2}} (\sigma_{xx}, \sigma_{yy}, \sigma_{xy}) z\, dz, \quad (19)$$

$$\left(M_{xxS}, M_{yyS}, M_{xyS}\right) = -\int_{-\frac{h}{2}}^{\frac{h}{2}} (\sigma_{xx}, \sigma_{yy}, \sigma_{xy}) f\, dz, \quad (20)$$

$$\left(Q_x, Q_y\right) = \int_{-\frac{h}{2}}^{\frac{h}{2}} (\sigma_{xz}, \sigma_{yz})\, \mathrm{g}\, dz, \quad (21)$$

The kinetic energy of plate can be written as

$$K = \frac{1}{2}\rho\int_A \int_{-\frac{h}{2}}^{\frac{h}{2}} \left(\left(\frac{\partial U_1}{\partial t}\right)^2 + \left(\frac{\partial U_2}{\partial t}\right)^2 + \left(\frac{\partial U_3}{\partial t}\right)^2\right) \mathrm{dz\, dA}. \quad (22)$$

where ρ is the density of structure.

The external work due to surrounding orthotropic visco-Pasternak medium can be written as

$$W = -\int_A (q) u_3\, dA, \quad (23)$$

where

$$\begin{aligned} q = {} & kw + c_d\dot{w} - G_\xi\left(\cos^2\theta w_{,xx} + 2\cos\theta\sin\theta w_{,yx} + \sin^2\theta w_{,yy}\right) \\ & - G_\eta\left(\sin^2\theta w_{,xx} - 2\sin\theta\cos\theta w_{,yx} + \cos^2\theta w_{,yy}\right), \end{aligned} \quad (24)$$

where angle θ describes the local ξ direction of orthotropic foundation with respect to the global x-axis of the plate; k, G_ξ and G_η are Winkler foundation parameter, shear foundation parameters in ξ and η directions, respectively. Finally, applying Hamilton's principle, the motion equations can be obtained as

$$\frac{\partial}{\partial x}N_{xx} + \frac{\partial}{\partial y}N_{xy} - I_0\frac{\partial^2 U}{\partial t^2} + I_1\frac{\partial^3 W_b}{\partial x \partial t^2} + J_1\frac{\partial^3 W_s}{\partial x \partial t^2} = 0, \quad (25)$$

$$\frac{\partial}{\partial x}N_{xy} + \frac{\partial}{\partial y}N_{yy} - I_0\frac{\partial^2 V}{\partial t^2} + I_1\frac{\partial^3 W_b}{\partial y \partial t^2} + J_1\frac{\partial^3 W_s}{\partial y \partial t^2} = 0, \quad (26)$$

$$\begin{aligned} & \frac{\partial^2}{\partial x^2}M_{xxB} + 2\frac{\partial^2}{\partial x\,\partial y}M_{xyB} + \frac{\partial^2}{\partial y^2}M_{yyB} + q \\ & + N_x^m\left(\frac{\partial^2 W_b}{\partial x^2} + \frac{\partial^2 W_s}{\partial x^2}\right) + N_y^m\left(\frac{\partial^2 W_b}{\partial y^2} + \frac{\partial^2 W_s}{\partial y^2}\right) \\ & - I_0\left(\frac{\partial^2 W_b}{\partial t^2} + \frac{\partial^2 W_s}{\partial t^2}\right) - I_1\left(\frac{\partial^3 U}{\partial x\,\partial t^2} + \frac{\partial^3 V}{\partial y\,\partial t^2}\right) \\ & + I_2\left(\frac{\partial^4 W_b}{\partial x^2\partial t^2} + \frac{\partial^4 W_b}{\partial y^2\partial t^2}\right) + J_2\left(\frac{\partial^4 W_s}{\partial x^2\partial t^2} + \frac{\partial^4 W_s}{\partial y^2\partial t^2}\right) = 0, \end{aligned} \quad (27)$$

$$\begin{aligned} & \frac{\partial^2}{\partial x^2}M_{xxS} + 2\frac{\partial^2}{\partial x\,\partial y}M_{xyS} + \frac{\partial^2}{\partial y^2}M_{yyS} + \frac{\partial}{\partial x}Q_x + \frac{\partial}{\partial y}Q_y \\ & + q + + N_x^m\left(\frac{\partial^2 W_b}{\partial x^2} + \frac{\partial^2 W_s}{\partial x^2}\right) + N_y^m\left(\frac{\partial^2 W_b}{\partial y^2} + \frac{\partial^2 W_s}{\partial y^2}\right) \\ & - I_0\left(\frac{\partial^2 W_b}{\partial t^2} + \frac{\partial^2 W_s}{\partial t^2}\right) - J_1\left(\frac{\partial^3 U}{\partial x\,\partial t^2} + \frac{\partial^3 V}{\partial y\,\partial t^2}\right) \\ & + J_2\left(\frac{\partial^4 W_b}{\partial x^2\partial t^2} + \frac{\partial^4 W_b}{\partial y^2\partial t^2}\right) + K_2\left(\frac{\partial^4 W_s}{\partial x^2\partial t^2} + \frac{\partial^4 W_s}{\partial y^2\partial t^2}\right) = 0, \end{aligned} \quad (28)$$

where the mass inertias can be defined as

$$\left(I_0, I_1, I_2, J_1, J_1, K_2\right) = \int_{-\frac{h}{2}}^{\frac{h}{2}} \rho\left(1, z, f, zf, z^2, f^2\right) dz. \quad (29)$$

By substituting Eqs. (11)-(15) into Eqs. (18)-(21) the stress resultants are obtained as

$$\begin{aligned} N_{xx} = {} & A_{11}\frac{\partial}{\partial x}U - A_{11z}\frac{\partial^2}{\partial x^2}W_b - A_{11f}\frac{\partial^2}{\partial x^2}W_s \\ & + A_{12}\frac{\partial}{\partial y}V - A_{12z}\frac{\partial^2}{\partial y^2}W_b - A_{12f}\frac{\partial^2}{\partial y^2}W_s, \end{aligned} \quad (30)$$

$$N_{yy} = A_{21}\frac{\partial}{\partial x}U - A_{21z}\frac{\partial^2}{\partial x^2}W_b - A_{21f}\frac{\partial^2}{\partial x^2}W_s + A_{22}\frac{\partial}{\partial y}V - A_{22z}\frac{\partial^2}{\partial y^2}W_b - A_{22f}\frac{\partial^2}{\partial y^2}W_s, \quad (31)$$

$$N_{xy} = A_{44}\frac{\partial}{\partial y}U + A_{44}\frac{\partial}{\partial x}V - 2A_{44z}\frac{\partial^2}{\partial x\,\partial y}W_b - 2A_{44f}\frac{\partial^2}{\partial x\,\partial y}W, \quad (32)$$

$$Q_x = A_{55g}\frac{\partial}{\partial x}W_s, \quad (33)$$

$$Q_y = A_{66g}\frac{\partial}{\partial y}W_s, \quad (34)$$

$$M_{xxB} = A_{11z}\frac{\partial}{\partial x}U - B_{11}\frac{\partial^2}{\partial x^2}W_b - A_{11zf}\frac{\partial^2}{\partial x^2}W_s + A_{12z}\frac{\partial}{\partial y}V - B_{12}\frac{\partial^2}{\partial y^2}W_b - A_{12zf}\frac{\partial^2}{\partial y^2}W_s +, \quad (35)$$

$$M_{xxS} = A_{11f}\frac{\partial}{\partial x}U - A_{11zf}\frac{\partial^2}{\partial x^2}W_b - E_{11}\frac{\partial^2}{\partial x^2}W_s + A_{12f}\frac{\partial}{\partial y}V - A_{12zf}\frac{\partial^2}{\partial y^2}W_b - E_{12}\frac{\partial^2}{\partial y^2}W_s, \quad (36)$$

$$M_{yyB} = A_{21z}\frac{\partial}{\partial x}U - B_{21}\frac{\partial^2}{\partial x^2}W_b - A_{21zf}\frac{\partial^2}{\partial x^2}W_s + A_{22z}\frac{\partial}{\partial y}V - B_{22}\frac{\partial^2}{\partial y^2}W_b - A_{22zf}\frac{\partial^2}{\partial y^2}W_s, \quad (37)$$

$$M_{yyS} = A_{21f}\frac{\partial}{\partial x}U - A_{21zf}\frac{\partial^2}{\partial x^2}W_b - E_{21}\frac{\partial^2}{\partial x^2}W_s + A_{22f}\frac{\partial}{\partial y}V - A_{22zf}\frac{\partial^2}{\partial y^2}W_b - E_{22}\frac{\partial^2}{\partial y^2}W_s, \quad (38)$$

$$M_{xyB} = 2A_{44z}\frac{\partial}{\partial y}U + 2A_{44z}\frac{\partial}{\partial x}V - 2B_{44}\frac{\partial^2}{\partial x\,\partial y}W_b - 2A_{44zf}\frac{\partial^2}{\partial x\,\partial y}W_s, \quad (39)$$

$$M_{xyS} = 2A_{44f}\frac{\partial}{\partial y}U + 2A_{44f}\frac{\partial}{\partial x}V - 2A_{44zf}\frac{\partial^2}{\partial x\,\partial y}W_b - 2E_{44}\frac{\partial^2}{\partial x\,\partial y}W, \quad (40)$$

where

$$(A_{11}, A_{12}, A_{22}, A_{44}) = \sum_{k=1}^{N}\int_{z^{(k-1)}}^{z^{(k)}}\left(C_{11}^{(k)}, C_{12}^{(k)}, C_{22}^{(k)}, C_{44}^{(k)}\right)dz, \quad (41)$$

$$(A_{11z}, A_{12z}, A_{22z}, A_{44z}) = \sum_{k=1}^{N}\int_{z^{(k-1)}}^{z^{(k)}}\left(C_{11}^{(k)}, C_{12}^{(k)}, C_{22}^{(k)}, C_{44}^{(k)}\right)z\,dz, \quad (42)$$

$$(A_{11f}, A_{12f}, A_{22f}, A_{44f}) = \sum_{k=1}^{N}\int_{z^{(k-1)}}^{z^{(k)}}\left(C_{11}^{(k)}, C_{12}^{(k)}, C_{22}^{(k)}, C_{44}^{(k)}\right)f\,dz, \quad (43)$$

$$(A_{11zf}, A_{12zf}, A_{22zf}, A_{44zf}) = \sum_{k=1}^{N}\int_{z^{(k-1)}}^{z^{(k)}}\left(C_{11}^{(k)}, C_{12}^{(k)}, C_{22}^{(k)}, C_{44}^{(k)}\right)zf\,dz, \quad (44)$$

$$(A_{55g}, A_{66g}) = \sum_{k=1}^{N}\int_{z^{(k-1)}}^{z^{(k)}}\left(C_{55}^{(k)}, C_{66}^{(k)}\right)dz, \quad (45)$$

$$(B_{11}, B_{12}, B_{22}, B_{44}) = \sum_{k=1}^{N}\int_{z^{(k-1)}}^{z^{(k)}}\left(C_{11}^{(k)}, C_{12}^{(k)}, C_{22}^{(k)}, C_{44}^{(k)}\right)z^2\,dz, \quad (46)$$

$$(E_{11}, E_{12}, E_{22}, E_{44}) = \sum_{k=1}^{N}\int_{z^{(k-1)}}^{z^{(k)}}\left(C_{11}^{(k)}, C_{12}^{(k)}, C_{22}^{(k)}, C_{44}^{(k)}\right)f^2\,dz, \quad (47)$$

5. GDQM

In this method, the differential equations are changed into a first order algebraic equation by employing appropriate weighting coefficients. Because weighting coefficients do not relate to any special problem and only depend on the grid spacing. In other words, the partial derivatives of a function (say w here) are approximated with respect to specific variables (say x and y), at a discontinuous point in a defined domain ($0 < x < L_x$ and $0 < y < L_y$) as a set of linear weighting coefficients and the amount represented by the function itself at that point and other points throughout the domain. The approximation of the n^{th} and m^{th} derivatives function with respect to x and y, respectively may be expressed in general form as (Lei *et al.* 2013)

$$f_x^{(n)}(x_i, y_i) = \sum_{k=1}^{N_x} A^{(n)}{}_{ik}\, f(x_k, y_j),$$
$$f_y^{(m)}(x_i, y_i) = \sum_{l=1}^{N_y} B^{(m)}{}_{jl}\, f(x_i, y_l), \quad (49)$$
$$f_{xy}^{(n+m)}(x_i, y_i) = \sum_{k=1}^{N_x}\sum_{l=1}^{N_y} A^{(n)}{}_{ik} B^{(m)}{}_{jl}\, f(x_k, y_l),$$

where N_x and N_y, denotes the number of points in x and y directions, $f(x, y)$ is the function and A_{ik}, B_{jl} are the weighting coefficients.

However, the motion equations can be written as

$$\left\{[K][d] + [C][\dot{d}] + [M][\ddot{d}]\right\} = [0], \quad (50)$$

6. Results and discussion

A computer program is prepared for the numerical solution of frequency of smart concrete plate resting on an orthotropic foundation.

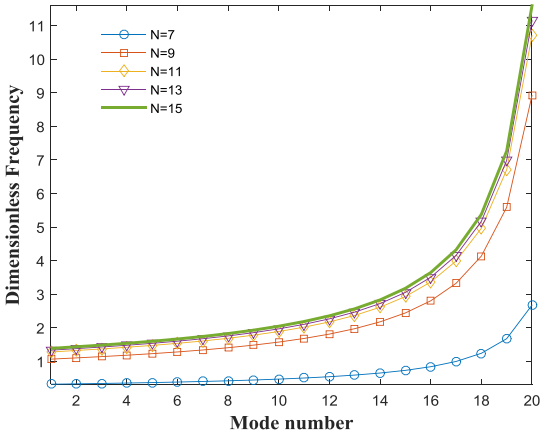

Fig. 2 Convergence of proposed method (DQM)

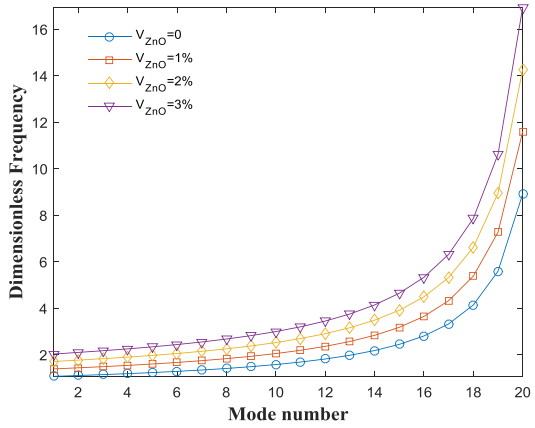

Fig. 3 ZnO Volume percent effects on the frequency

The convergence and accuracy of the DQM in calculating the frequency of the smart concrete plate is shown in Fig. 2. Fast rate of convergence of the method are quite evident and it is found that 15 DQ grid points can yield accurate results.

In realizing the influence of ZnO as reinforce, Fig. 3 is plotted. This figure shows the effects of ZnO volume fraction on the dimensionless frequency ($\Omega = \omega(a/h)^2\sqrt{\rho(1-\upsilon^2)/E}$) with respect to mode number. As can be seen, with increasing the ZnO volume fraction, the frequencies are increased. It is due to increase in the stiffness of structure.

The effect of different boundary conditions is presented in Fig. 4 on the dimensionless frequency versus mode number. It can be found that the CCCC boundary condition yields to higher frequency. In other words, comparing the assumed boundary conditions, the frequency is maximum for CCCC boundary conditions.

Figs. 5 and 6 demonstrate the effects of length to width ratio and length to thickness ratio on the dimensionless frequency versus mode number, respectively. As can be seen, the frequency of the system decreases with increasing length to width ratio and increases with increasing length to thickness ratio. It since the stiffness of the structure increase with increasing length to thickness ratio.

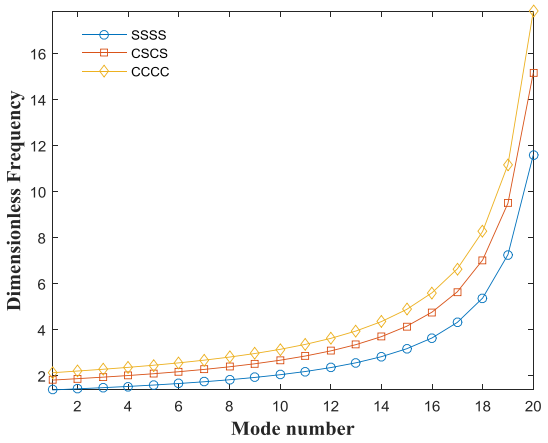

Fig. 4 Boundary condition effects on the frequency

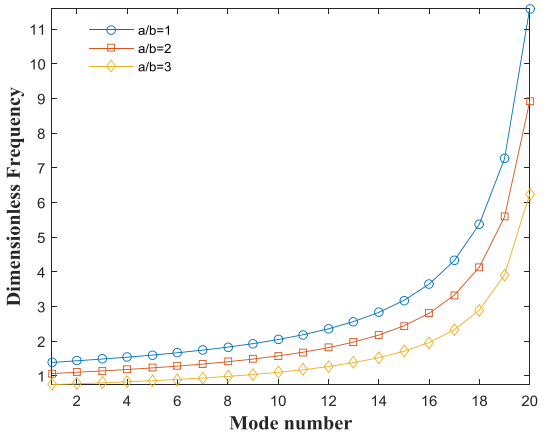

Fig. 5 The effect of length to width ratio on the dimensionless frequency

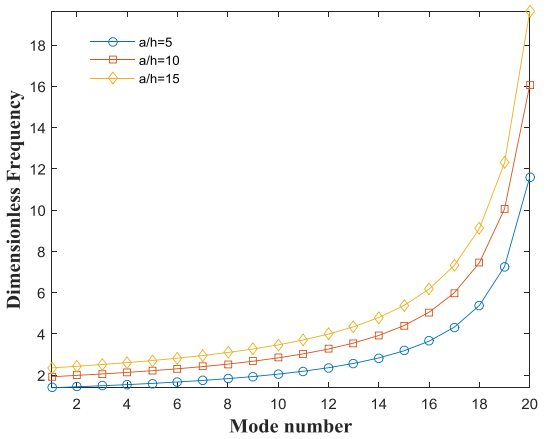

Fig. 6 The effect of length to thickness ratio on the dimensionless frequency

7. Conclusions

Vibration of smart concrete plate was presented. The plate is reinforced with ZnO which the equivalent material properties were obtained by mixture model. Orthotropic foundation was used for simulating the surrounding elastic medium. The SSDT was applied for mathematical modeling of structure. DQ was applied for obtaining the frequency of structure so that the effects of different parameters such as volume percent of ZnO, boundary conditions and geometrical parameters were shown. As can be seen, with increasing the ZnO volume fraction, the frequencies were increased. It can be found that the CCCC boundary condition yields to higher frequency. As can be seen, the frequency of the system decreases with increasing length to width ratio and increases with increasing length to thickness ratio.

References

Abdollahzadeh Shahrbabaki, E. and Alibeigloo, A. (2014), "Three-dimensional free vibration of carbon nanotube-reinforced composite smart concrete plate with various boundary conditions using Ritz method", *Compos. Struct*., **111**, 362-370.

Atteshamuddin, S.S. and Yuwaraj, M.Gh. (2017), "On the free vibration of angle-ply laminated composite and soft core smart concrete plate", *Int. J. Sandw. Struct*., In press.

Chetan, S.J., Madhusudan, M., Vidyashankar, S. and Charles Lu, Y. (2017), "Modelling of the interfacial damping due to nanotube agglomerations in nanocomposites", *Smart Struct. Syst*., **19**(1), 57-66.

Ke, L.L., Liu, C. and Wang, Y.S. (2015), "Free vibration of piezoelectric nanosmart concrete plate under various boundary conditions", *Physica E*, **66**, 93-106.

Kiani, K. (2014), „Free vibration of conducting nanosmart concrete plate exposed to unidirectional in-plane magnetic fields using shear deformable plate theories", *Physica E*, **57**, 179-192.

Lanhe, W., Wang, H. and Wang, D. (2007), "Dynamic stability analysis of FGM smart concrete plate by the moving leastsquares differential quadrature method", *Compos. Struct*., **77**, 383-394.

Lei, Y., Adhikari, S. and Friswell, M.I. (2013), "Vibration of Kelvin–Voigt damped Timoshenko beams", *Int. J. Eng. Sci*., **66-67**, 1-13.

Li, Y.S., Cai, Z.Y. and Shi, S.Y. (2014), "Buckling and free vibration of magnetoelectroelastic nanoplate based on theory", *Compos. Struct*., **111**, 522-529.

Mantari, J.L. and Guedes Soares, C. (2014), "Four-unknown quasi-3D shear deformation theory for advanced composite smart concrete plate", *Compos. Struct*., **109**, 231-239.

Mori, T. and Tanaka, K. (1973), "Average stress in matrix and average elastic energy of materials with misfitting inclusions", *Acta Metal. Mater*., **21**, 571-574.

Natarajan, S., Haboussi, M. and Manickam, G. (2014), "Application of higher-order structural theory to bending and free vibration analysis of smart concrete plate with CNT reinforced composite facesheets", *Compos. Struct*., **113**, 197-207.

Pandit, M.K., Sheikh, A.H. and Singh, B.N. (2009), "Analysis of laminated smart concrete plate based on an improved higher order zigzag theory", *Int. J. Sandw. Struct.*, **12**, 307-326.

Phung-Van, P., Abdel-Wahab, M. and Liew, K.M. (2017), "Isogeometric analysis of carbon nanotube-reinforced composite smart concrete plate using higher-order shear deformation theory", *Compos. Struct*., **123**, 137-149.

Rafiee, M., He, X.Q. and Liew, K.M. (2014), "Non-linear dynamic stability of piezoelectric carbon nanotube-reinforced composite smart concrete plate with initial geometric imperfection", *Int. J. Nonlinear Mech.*, **59**, 37-51.

Shen, H.S. (2009), "Nonlinear bending of carbon nanotube-reinforced composite smart concrete plate in thermal environments", *Compo. Struct*., **91**, 9-19.

Thai, H.T. and Vo, T.P. (2013), "A new sinusoidal shear deformation theory for bending buckling and vibration of smart concrete plate", *Appl. Math. Model*., **37**, 3269-3281.

Wattanasakulpong, N. and Chaikittiratana, A. (2015), "Exact solutions for static and dynamic analyses of carbon nanotube-reinforced composite smart concrete plate with Pasternak elastic foundation", *Appl. Math. Model*., **9**, 5459-5472.

Ying, Z.G., Ni, Y.Q. and Duan, Y.F. (2017), "Stochastic micro-vibration response characteristics of a plate with MR visco-elastomer core and mass", *Smart Struct. Syst.*, **16**(1), 141-162.

CC